Integrated State & Topology Estimation Based on *A Priori* Topology Information

Victor Freitas
Antonio Simões Costa
Power Systems Group
Federal University of Santa Catarina
Florianpolis, SC, Brazil
victor.silva@posgrad.ufsc.br simoes@labspot.ufsc.br

***Abstract*—This paper addresses the simultaneous estimation of state variables and network topology in the context of power system real-time modeling. The proposed method assumes that selected substations are modeled at the bus section level, and circuit breakers and disconnects are explicitly represented. Available information on the statuses of such switching branches are then treated as *a priori* topology information to be processed by a specialized estimator. The presumed topology will eventually be either validated or corrected by using the information conveyed by real-time measurements. An algorithm based on a fast version of orthogonal Givens rotations is employed to solve the integrated state & topology estimation problem. The proposed method preserves the bad data processing capabilities of weighted least-squares state estimators. The performance of the integrated state & topology estimator is assessed through its application to test systems derived from IEEE benchmark networks.**

***Index Terms*—Power System State and Topology Estimation; Power System Real-Time Modeling.**

I. Introduction

Power system real-time modeling relies basically on two classes of data: measurements of analog quantities gathered by SCADA and phasor measurement units, and the network topology. The latter is provided by the Network Configurator, which in turn processes digital measurements related to circuit breaker statuses. Topology determination constitutes the basic step from which the various state estimation components become able to process the analog measurements and eventually provide the state estimates.

Both analog and digital measurements may occasionally become contaminated by gross errors. In the former case, efficient methods performed at bus-branch level have been developed in the past in order to reject bad data and thus to prevent their influence on the final estimates [1]. Errors on digital measurements, although less frequent, may also occur, and their consequences tend to be more serious than those caused by analog gross measurements. Since topology errors are difficult to trace down when conventional bus-branch models are employed, generalized state estimation methods relying on network representation at the bus section level have been on the rise since the early nineties [1]. As a consequence, a number of distinct approaches to deal with uncertain topology have been proposed, such as the development of new EMS functions specifically intended to perform topology estimation [2]. Other methods rely on a constrained optimization framework for state estimation in which circuit breaker statuses appear as equality constraints [3].

This paper builds on previous contributions that represent at bus section level portions of the network suspect of containing modeling errors [1]–[3]. In addition, the proposed approach relies on the recognition that analog measurements intrinsically contain information related to the network topology. The latter observation is not usually exploited in conventional power system real-time modeling, which sees topology determination and state estimation as completely disjointed processes. The joint state & topology estimation rationale used in this paper has only recently been explored in the literature [4]–[7].

The proposed methodology is capable of extracting topology information from analog measurements while simultaneously estimating the node voltages. Such an integrated state and topology estimation framework treats the output of the Network Configurator as *a priori* topology information, what is made possible by modeling the relevant portion of the network at bus section level. An orthogonal estimation algorithm able to process *a priori* state information is employed to solve the integrated state and topology estimation problem and to process analog bad data. An important feature of the proposed approach is that the level of uncertainty assigned to presumed topologies can be statistically characterized, thereby facilitating the conception of hypothesis testing strategies for bad data processing.

This paper is organized as follows. Section II presents the background. The integrated state & topology modeling is dealt with in Section III. Topology validation and bad data processing are discussed in Sections IV and V, respectively. Numerical results from different cases simulated on the IEEE 14-bus test system are presented in Section VI. Finally, Section VII presents the concluding remarks.

II. Theoretical Background

A. Modeling Power Systems at Bus Section Level

After conventional state estimation indicates the presence of modeling errors within a region of the power network, we assume that the suspect substations are modeled at bus section level, whereas the sound subnetwork remains represented at

The second author acknowledges the financial support of the Brazilian National Research Council (CNPQ)

bus-branch level [2], [3], [5], [7]. This implies that the state vector is augmented by taking the active and reactive power flows through circuit breakers as new state variables [1]. In this paper, the latter are referred to as *flow states*, as opposed to the conventional *nodal states* (angles and magnitudes of nodal voltage). Thus, if the suspected substations comprise n_{sb} switching branches, $2n_{sb}$ new state variables are included in the model. Since the state vector $\mathbf{x}$ also contains the conventional nodes states for the *N* network nodes, the dimension of $\mathbf{x}$ becomes $n = 2N + 2n_{sb} - 1$.

The status of switching branches is modeled as follows: closed switching branches imply zero complex voltage drop across the branch terminals, i.e.

$$\delta_i - \delta_j = 0 \quad ; \quad V_i - V_j = 0. \tag{1}$$

On the other hand, an open switching branch is characterized by zero active and reactive power flows through it, i.e.

$$p_{ij} = 0 \quad ; \quad q_{ij} = 0. \tag{2}$$

The relationships in (1) and (2) are referred to as *operational conditions*, and are collectively represented by

$$\mathbf{h_o}(\mathbf{x}) = \mathbf{0}. \tag{3}$$

Furthermore, zero injection nodes are modeled as equality constraints, referred to as *structural constraints* and represented by the following set of nonlinear equations:

$$\mathbf{h_s}(\mathbf{x}) = \mathbf{0}. \tag{4}$$

Finally, the measurement model relates measured quantities and state variables, and is given by:

$$\begin{array}{l} \mathbf{z_m} = \mathbf{h_m}(\mathbf{x}) + \boldsymbol{\eta_m} \\ E\{\boldsymbol{\eta_m}\} = \mathbf{0} \qquad\quad ; \quad E\{\boldsymbol{\eta_m}\boldsymbol{\eta_m}^T\} = \mathbf{R_m} \end{array} \tag{5}$$

where $\mathbf{h_m}(\mathbf{x})$ is an $m \times 1$ vector of nonlinear functions and $\eta_\mathbf{m}$ is an $m \times 1$ measurement error vector, assumed to be normally distributed, with zero mean and an $m \times m$ covariance diagonal matrix, denoted by $\mathbf{R_m}$.

B. Power System State Estimation Considering A Priori *State Information*

A priori information on the state variables can be modeled in the state estimation problem as an extra quadratic term added to the weighted least squares criterion [8]. The equality structural constraints are inserted into the problem as pseudo-measurements of high accuracy. Thus, the Power System State Estimation (PSSE) problem is formulated as:

$$\begin{array}{ll} \mathit{Minimize} & J(\hat{\mathbf{x}}) = \mathbf{r}^T\mathbf{R}^{-1}\mathbf{r} + (\hat{\mathbf{x}} - \bar{\mathbf{x}})^T\boldsymbol{\Sigma}^{-1}(\hat{\mathbf{x}} - \bar{\mathbf{x}}) \\ \mathit{Subject\ to} & \mathbf{r} = \mathbf{z} - \mathbf{h}(\hat{\mathbf{x}}) \end{array} \tag{6}$$

where

$$\begin{array}{l} \mathbf{z} = [\mathbf{z_m}^T, \mathbf{0}]^T \quad ; \quad \mathbf{h} = [\mathbf{h_m}(\hat{\mathbf{x}})^T, \mathbf{h_s}(\hat{\mathbf{x}})^T]^T; \\ \mathbf{R} = diag\{\mathbf{R_m}, \mathbf{R_s}\} \qquad\qquad . \end{array} \tag{7}$$

In (6), $\boldsymbol{\Sigma}$ is the covariance matrix of the *a priori* state values $\bar{\mathbf{x}}$ and $\mathbf{R_s}$ is the diagonal covariance matrix of the structural constraints [9]. Theoretically, $\mathbf{R_s}$ is a null matrix as it correspond to deterministic information. However, in order to avoid numerical problems in the convergence process, it is often convenient to make $\mathbf{R_s}$ equal to $\varepsilon_s\mathbf{I}$, where $\mathbf{I}$ stands for the identity matrix of appropriate dimension and the positive number ε_s is chosen as some orders of magnitude less than typical measurement variances. Operational conditions $\mathbf{h_o}(\hat{\mathbf{x}})$ that model the presumed topology will be dealt with as *a priori* information, as discussed in Section III.

If a nonlinear model is used to represent the electric network, the solution of problem (6) can be obtained through Gauss-Newton method, which leads to the following extended version of the Normal Equation [10]:

$$[\mathbf{H^T R^{-1} H} + \boldsymbol{\Sigma}^{-1}]\boldsymbol{\Delta x} = \mathbf{H^T R^{-1}}\boldsymbol{\Delta z} + \boldsymbol{\Sigma}^{-1}\boldsymbol{\Delta}\bar{\mathbf{x}} \tag{8}$$

where $\mathbf{H}$ is the Jacobian matrix of $\mathbf{h}(\mathbf{x})$ computed at a given point $\mathbf{x}^k$, $\boldsymbol{\Delta z} = \mathbf{z} - \mathbf{h}(\mathbf{x}^k)$ and $\boldsymbol{\Delta}\bar{\mathbf{x}} = \bar{\mathbf{x}} - \mathbf{x}^k$. The solution of (8) provides the incremental state vector $\boldsymbol{\Delta x}$. The estimated states are then iteratively updated as:

$$\mathbf{x}^{(k+1)} = \mathbf{x}^{(k)} + \boldsymbol{\Delta x}. \tag{9}$$

The iterative process goes on until $\boldsymbol{\Delta x}$ becomes smaller than a pre-specified tolerance.

III. Integrated State & Topology Modeling

A. Enforcing Topology Conditions as A Priori *Information: the Outer Adjustment Method*

The network topology validation method proposed in this paper is aimed at extracting topology information from the analog measurements available to the state estimator. Accordingly, results provided by the Network Processor are seen as an initially presumed topology, which must then be confirmed or revised by the proposed joint state & topology estimator. This is accomplished by translating the Network Configurator outcome into operational conditions, made available to the estimator as entries of vector $\bar{\mathbf{x}}$ prior to the real-time measurement processing stage. Such a process of converting the presumed topology into operational conditions is carried out at the beginning of each iteration of the nonlinear estimation solution, as follows:

a) At the first iteration, *a priori* state information is defined as the flat start for all nodal states, and zero values for all active and reactive switching branch *flow states*;

b) Beginning at the second iteration, switching branch statuses consistent with the Network Processor results are enforced, as detailed next:

i) A closed switching branch connecting substations internal nodes *i* and *j* leads to the following definition of a *a priori* state values:

$$\delta_i^{(k+1)} = \delta_j^{(k)} \quad ; \quad V_i^{(k+1)} = V_j^{(k)}, \quad k = 1, 2, ... \tag{10}$$

ii) An open status of a switching branch whose terminal nodes are *i* and *j* is taken into account by initialing the corresponding flow states in $\bar{\mathbf{x}}$ as :

$$p_{ij}^{(k+1)} = 0 \quad ; \quad q_{ij}^{(k+1)} = 0, \quad k = 1, 2, ... \tag{11}$$

Finally a covariance matrix $\mathbf{\Sigma}$ must be assigned to the *a priori* state information. As shown in (6), the inverse of $\mathbf{\Sigma}$ plays the role of a weighting matrix in the objective function, establishing the relative importance of *a priori* topology information with respect to the measurements in the estimation process. In this paper, we rely on such interpretation to define $\mathbf{\Sigma}$ as a function of the measurement covariance matrix, as follows:

$$\Sigma_{ii} = \bar{R}_{m,ii}/k_w \tag{12}$$

where $\bar{R}_{m,ii}$ is the mean value of the measurement variances, and k_w is a positive valued calibrating parameter. Extensive experiments conducted with distinct test system indicate that values in the range $0 < k_w < 1$ yield proper results, although upper range values tend to increase the number of iterations for convergence. In this paper, we use $k_w = 0.025$.

We refer to the method for initializing information given by (10) and (11) as the *outer adjustment method*, since topology conditions are enforced outside each iteration of the estimation process. This approach is algorithm-independent, in the sense that it does not rely on specific properties of a given algorithm.

B. PSSE Solution through Givens Rotations

PSSE solution methods based on fast version of orthogonal of Givens Rotations have proven to be both numerically robust and effective [11], [12]. In this paper, we solve the weighted least-squares problem (6) through the three-multiplier version of Givens rotations (G3M) [13], instead of using the extend normal equation (8). To outline the algorithm, consider that successive orthogonal transformations are applied to matrix $\mathbf{H}$ and vector $\mathbf{z}$ (both previously scaled by matrix $\mathbf{R}^{-\frac{1}{2}}$) in order to obtain an upper triangular linear system of equations. If $\mathbf{Q}$ represents the matrix that cumulatively stores the individual rotations, we have:

$$\mathbf{Q}\ (\mathbf{R}^{-\frac{1}{2}}\ [\ \mathbf{H}\ \ |\ \ \mathbf{z}\ ]) = \left[\begin{array}{c|c} \mathbf{U} & \mathbf{c} \\ 0 & d \end{array}\right] \tag{13}$$

where $\mathbf{U}$ is an upper $n \times n$ triangular matrix and $\mathbf{c}$ is a $n \times 1$ vector. The fast version of Givens rotations are based on the decomposition of matrix $\mathbf{U}$ as [11], [13]:

$$\mathbf{U} = \mathbf{D}^{\frac{1}{2}}\bar{\mathbf{U}} \tag{14}$$

where $\mathbf{D}$ is a diagonal weighting matrix and $\bar{\mathbf{U}}$ is a unit upper triangular matrix. Since vector $\mathbf{z}$ is considered as an extra column of $\mathbf{H}$, the resulting vector $\mathbf{c}$ is also scaled in the transformation, and is then denoted by $\bar{\mathbf{c}}$. The inclusion of scaling factors is attractive because it eliminates square-root computations during the factorizations given by (13) [13]. In practice, $\mathbf{D}^{-\frac{1}{2}}$ is never required, and only $\mathbf{D}$ needs to be computed.

Following the transformations step given by (14), the vector of increments $\mathbf{\Delta x}$ is obtained by simple solving the upper triangular system

$$\bar{\mathbf{U}}\mathbf{\Delta x} = \bar{\mathbf{c}} \tag{15}$$

by back-substitution. The weighted sum of squared residuals is determined from d, as a by-product of the estimation process.

We can take advantage of the above scaling mechanism to assign weights to both initial values of state variables *and* the presumed topology before any measurement is processed, with no extra computational cost. This is described in the sequel.

In practice, the state estimation problem with *a priori* state information is initialized as

$$\bar{\mathbf{U}}^{(0)}\mathbf{x}^{(0)} = \bar{\mathbf{c}}^{(0)} \tag{16}$$

where $\bar{\mathbf{U}}^{(0)}$ is an upper triangular matrix whose diagonal entries are equal to 1 and off-diagonal entries are all zeroes; vector $\bar{\mathbf{c}}^{(0)}$ contains the values assigned to *a priori* state information and $\mathbf{x}^{(0)}$ is the initial state vector. Furthermore, the entries of diagonal weighting matrix $\mathbf{D}$ are given by $d_{ii} = 1/\Sigma_{ii}$ [10].

In addition to other desired properties, G3M provides means to take into account topology validation and bad data detection/identification in the course of the state estimation process. Such features will be discussed in next subsections.

C. Network Topology Representation using Matrix $\bar{\mathbf{U}}^0$: the Inner Adjustment Method

When G3M is selected as the state estimation algorithm, an alternative arises to the Outer Adjustment Method of Section III-A for modeling the presumed topology. It basically consists in directly representing the topology in the initial matrix $\bar{\mathbf{U}}^0$, as well as assigning the initial row weights $\mathbf{D}^0$ accordingly. The way $\bar{\mathbf{U}}^0$ is defined depends on the assumed status of each switching branch, as follows:

(i) An open switching branch ℓ whose terminal nodes are i and j is represented by initialing $\bar{\mathbf{U}}$ exactly as in (16); the entries of $\bar{\mathbf{c}}^0$ corresponding to the *flow states* p_{ij} and q_{ij} are made equal to zero, and the respective row weights in $\mathbf{D}$ are made equal to $1/\Sigma_{\ell\ell}$;

(ii) For a closed switching branch ℓ connecting nodes i and j, $j > i$, let k_i^δ (k_i^V) denote the state variable corresponding to nodal voltage angle δ_i (voltage magnitude V_i). To represent the closed breaker, the diagonal entries of $\bar{\mathbf{U}}^0$ are still as in (16), but now the two off-diagonal values $\bar{u}_{k_i^\delta,k_j^\delta}$ and $\bar{u}_{k_i^V,k_j^V}$ are both made equal to -1.

In addition, entries k_i^δ, k_j^δ, k_i^V and k_j^V of vector $\bar{\mathbf{c}}^0$ are made equal zero. Finally, the row weights for $\bar{\mathbf{U}}^0$ are defined as: $D_{k_i^\delta,k_i^\delta} = D_{k_i^V,k_i^V} = 1/\Sigma_{\ell\ell}$, and $D_{k_j^\delta,k_j^\delta} = D_{k_j^V,k_j^V} = 0$.

The rationale to define $\bar{\mathbf{U}}^0$ as above should be clear from (1), (2) and (16) for each of the two possible statuses. In case (ii), the definition of $\mathbf{D}$ is explained by the fact that a variance $\Sigma_{\ell\ell}$ is assigned to the voltage drop across the switching branch terminals, as given by (12). However, we assume that there is total uncertainty concerning the value of the voltage angle and magnitude at nodal j (assumption which, for that matter, is also made in this paper for all other nodal states).

IV. Topology Validation

Regardless whether topology *a priori* modeling is based on the inner or the outer adjustment method, the outcome of the integrated state & topology estimation procedure provides estimates for both nodal states and flow states. A post-processing

stage is then needed to either validate or make corrections on the initially presumed network topology. It basically consists of applying statistical tests to switching branch flow estimates. Specifically, uncertain breaker statuses are determined from the estimated switching branch power flow values through a hypothesis testing procedure based on a given significance level for the test, as previously proposed in [3]. From the specified significance level value and the variance of the error in the estimate for the flow states through a given switching branch ℓ, a threshold ε_{flow_ℓ} is determined, which is then used to decide whether the breaker is open or closed. Accordingly, if the absolute value of such estimated flow is greater than ε_{flow_ℓ}, one concludes that the corresponding breaker is closed; otherwise, the breaker is treated as open. In case devices with wrong presumed statuses are identified, the algorithm corrects them and a new integrated estimation is performed. This procedure is reapplied until no more changes are need.

As a final note, it should be mentioned that the covariance matrix on the estimation errors in the flow states required to compute each threshold ε_{flow_ℓ} can be obtained from matrices $\bar{\mathbf{U}}$ and $\mathbf{D}$ of the G3M estimator [11].

V. Bad Data Processing

Analog bad data processing is an essential attribute of any state estimator, and this also applies to the integrated state & topology estimator. The proposed bad data processing procedure relies on the following principles: (*i*) The *a priori* state information data related to the network topology can be seen as *virtual measurements*, since they are treated in the objective function (6) as a least squares term weighted by the inverse of the respective covariance matrix, that is, precisely in the same manner as ordinary measurements; (*ii*) As a consequence, the statistical properties of the solution are preserved, and available bad data processing tools previously developed for weighted least squares estimators are applicable in connection with the integrated estimator. In what follows, it is assumed that the available level of measurement redundancy is sufficient to allow the proper performance of conventional bad data processing methods.

The proposed bad data processing procedure is composed of two stages: gross error detection, based on the familiar $J(\hat{\mathbf{x}})$-test [1]; and bad data identification, based on the $\hat{b}$-test, applied to an estimate of the error magnitude of the measurement whose normalized residual is the largest [1]. In addition, advantage is taken of the fact that state estimation is carried out in this paper through the G3M method outlined in subsection III-B. As described in [11], this algorithm allows the monitoring of the $J(\hat{\mathbf{x}})$ value evolution and its comparison with the chi-square threshold [1] as the measurements are sequentially processed.

Whenever the $J(\hat{\mathbf{x}})$-test points out the occurrence of bad data, the $\hat{b}$-test is applied to the *analog measurement* whose normalized residual (r_i^N) is maximum. If the estimated error $\hat{b}$ of such measurement exceeds a pre-specified threshold (usually set as 4.0, see [1]), it is concluded that the analog measurement is erroneous, and it is removed from the measurement set. State estimation is restarted and the test is re-applied, until $\hat{b}$ satisfies the threshold.

On the other hand, if the first application of the $\hat{b}$-test is negative for errors in analog measurements, one concludes that the detected is due an incorrect presumed topology. Accordingly, no further action is taken at this stage, since the topology validation (see Section IV) executed as the next step of the estimation procedure takes care of extracting the correct topology from the available measurements.

The case studies reported in the following section illustrate the application of the above procedures.

VI. Simulation Results

The IEEE 14-bus network employed to assess the performance of the proposed method, and the corresponding metering scheme used in the reported case studies is shown in Fig. 1. The region composed by substations 6 and 13, as indicated in the figure, is randomly selected to simulate anomalies, which include topology errors and bad data in analog measurements. The bus-section level model of the related substations is detailed in Fig. 2. It can be seen that different circuit breaker arrangements are considered, such as double breaker, breaker-and-a-half and ring bus. A full nonlinear version of the algorithm has been implemented in Matlab, thus allowing the representation of both active and reactive power quantities, as well as complex bus voltages. Altogether, the state vector comprises 80 nodal and flow state variables. Measurement accuracies used to simulate the measurements and determine the corresponding variances are assumed to be 3×10^{-3} $p.u.$ for voltage magnitudes and 2×10^{-2} $p.u.$ for power flows and injections.

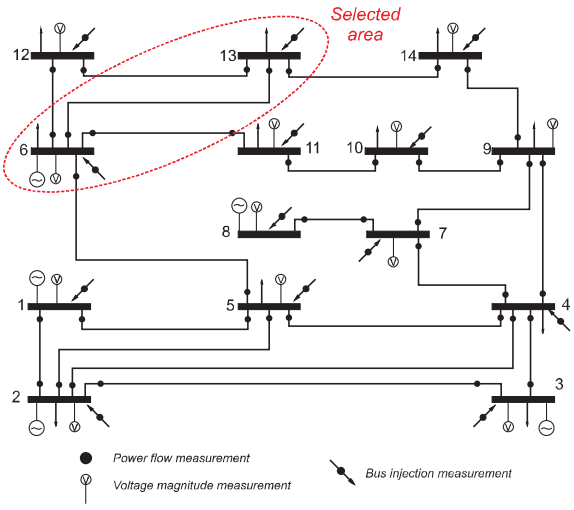

Fig. 1. IEEE 14-bus.

A. Presumed Topology Errors Only

This subsection presents the results obtained from the integrated state & topology estimation using both the outer and the inner adjustment methods discussed in Subsections III-A and III-C, respectively. In this case study, the statuses of three

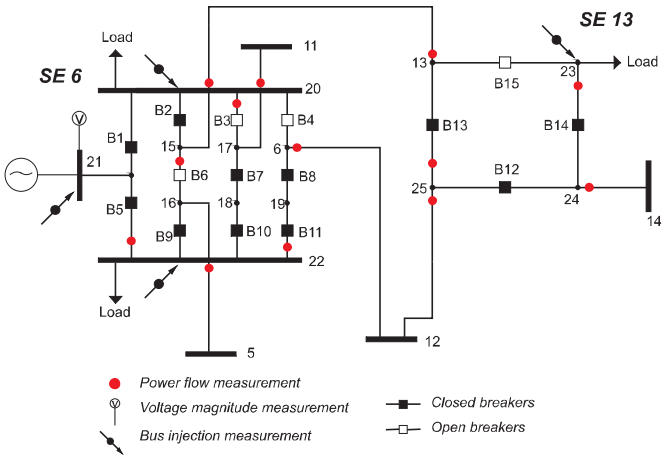

Fig. 2. Details of substations 6 and 13 of IEEE 14-bus.

circuit breakers (B2, B6 and B9, see Fig. 2) located on a single section of the breaker-and-half arrangement of substation 6 are erroneously inverted, that is, breakers B2 and B9 are assumed open and breaker B6 is closed. The resulting incorrect topology provided by de Network Configurator disconnects substation 6 from buses 5 and 13. Table I shows how the statuses of switching branches related to this case evolve through the iterative process, which takes two iterations to converge for both outer and inner adjustment methods. Table II presents the values of the objective function components computed in the end of the first iteration (that is, in the presence of the incorrect topology) and at convergence. The large initial values reflect the presence of the presumed topology error, which affects mostly the topology-related term.

TABLE I
SEQUENCE OF STATUS CHANGES THROUGH THE ITERATIONS

	B1	*B2*	*B3*	*B4*	*B5*	*B6*	*B7*	*B8*	*B9*
Correct Status	1	1	0	0	1	0	1	1	1
Presumed Status	1	*0*	0	0	1	*1*	1	1	*0*
Iteration 1	1	**1**	0	0	1	**0**	1	1	**1**
Iteration 2	1	**1**	0	0	1	**0**	1	1	**1**

TABLE II
OBJECTIVE FUNCTION COMPONENTS WITH PRESUMED TOPOLOGY ERROR ONLY

	Inner Adj. Method		*Outer Adj. Method*	
Objective Function	*Initial*	*Final*	*Initial*	*Final*
$J(\hat{\mathbf{x}})$	92.88	6.577	92.88	6.579
$\mathbf{r}^{\mathbf{T}}\mathbf{R}^{-\mathbf{1}}\mathbf{r}$	11.06	6.573	11.06	6.573
$(\bar{\mathbf{x}}-\hat{\mathbf{x}})^{\mathbf{T}}\boldsymbol{\Sigma}^{-\mathbf{1}}(\bar{\mathbf{x}}-\hat{\mathbf{x}})$	81.82	0.0038	81.82	0.0051

As soon as the statuses are corrected at the final iteration for both methods, objective function values undergo sharp reductions, as one would expect.

B. Simultaneous Topology and Analog Measurement Errors

This section presents the results obtained from the integrated state & topology estimator in the simultaneous presence of lack of knowledge on the network topology and a gross analog measurement error. Due to space limitations only one case related to this severe conditions is reported. The simulated gross analog measurement is the injection P_{23}, located at substation 13 (see Fig. 2) and the bad data size amounts to 15 standard deviations. Since the network topology is assumed completely unknown, all breaker statuses are initialized as "open", as show in Table V. Table III presents the measurement value with and without gross error, and Table IV summarizes the bad data processing stages. The gross error measurement is detected, identified and removed in the second iteration of the G3M algorithm and in the first one of the integrated state & topology estimation method. As shown in Table V, the latter takes two iterations to converge. Table IV also shows that both the outer and inner methods reach the same results for bad data processing. After the removal of the bad analog data, the $J(\hat{\mathbf{x}})$ value undergoes reduction, although it is still large due to the existence of topology errors. Those are checked and then corrected, and a next iteration is processed to validate the status changes, as shown in Table V. Finally, Table VI presents the values of the objective function components computed in the end of the first iteration (that is, in the presence of the incorrect topology but after the gross measurement removal) and at convergence.

TABLE III
SIMULATED GROSS ERRORS IN ANALOG MEASUREMENT

Erroneous Measurement	**Actual Value** $(p.u.)$	**Simulated Value** $(p.u.)$
P_{23}	-0.135	$+0.142$

TABLE IV
BAD DATA PROCESSING WITH SIMULTANEOUS TOPOLOGY ERRORS

Inner and Outer Adjustment Method					
Measur. Identified	r_i^N	$\hat{b}$	*G3M Iter.*	$J(\hat{\mathbf{x}})$ *Before*	$J(\hat{\mathbf{x}})$ *After*
P_{23}	8.559	12.948	2	264.33	177.05

TABLE V
SEQUENCE OF STATUS CHANGES THROUGH THE ITERATIONS

	B1	*B2*	*B3*	*B4*	*B5*	*B6*	*B7*	*B8*
Correct Status	1	1	0	0	1	0	1	1
Presumed Status	*0*	*0*	0	0	*0*	0	*0*	*0*
Iteration 1	**1**	**1**	0	0	**1**	0	**1**	**1**
Iteration 2	**1**	**1**	0	0	**1**	0	**1**	**1**

	B9	*B10*	*B11*	*B12*	*B13*	*B14*	*B15*
Correct Status	1	1	1	1	1	1	0
Presumed Status	*0*	*0*	*0*	*0*	*0*	*0*	0
Iteration 1	**1**	**1**	**1**	**1**	**1**	**1**	0
Iteration 2	**1**	**1**	**1**	**1**	**1**	**1**	0

TABLE VI
OBJECTIVE FUNCTION COMPONENTS WITH SIMULTANEOUS TOPOLOGY AND MEASUREMENT ERRORS

	Inner Adj. Method		*Outer Adj. Method*	
Objective Function	*Initial*	*Final*	*Initial*	*Final*
$J(\hat{\mathbf{x}})$	177.03	6.537	177.03	6.538
$\mathbf{r}^{\mathbf{T}}\mathbf{R}^{-\mathbf{1}}\mathbf{r}$	17.13	6.523	17.13	6.523
$(\bar{\mathbf{x}}-\hat{\mathbf{x}})^{\mathbf{T}}\boldsymbol{\Sigma}^{-\mathbf{1}}(\bar{\mathbf{x}}-\hat{\mathbf{x}})$	159.90	0.0140	159.90	0.0153

C. Gross Error in Analog Measurement Only

This subsection deals with the processing of a gross error in analog measurement located in a low redundancy area, considering that the presumed network topology is kept free of error. The purpose is to investigate the effect of low measurement redundancy on the proposed method's performance.

TABLE VII
SIMULATED GROSS ERROR IN ANALOG MEASUREMENT

Erroneous Measurement	*Actual Value (p.u.)*	*Simulated Value (p.u.)*
$p_{15\text{-}16}$	0.0	0.2019

Table VII shows the actual and simulated values of a particular active power flow measurement ($p_{15\text{-}16}$), which is directly associated to the flow in breaker B6. Despite the low local redundancy of the original Metering Scheme (referred to as M.S. 1 in Table VIII), integrated state & topology estimation is performed, and the results of both outer and inner adjustment methods are presented in rows corresponding to M.S. 1 of Table VIII. In all cases, bad data processing is carried out in the second iteration of the G3M algorithm. The detection threshold obtained from the chi-square distribution for a false alarm probability of 5% is $K = 129.92$. The results for metering scheme 1 in Table VIII show that the bad data is properly detected, but real power injection P_{20} is identified as the gross measurement instead of $p_{15\text{-}16}$. A closer examination of metering scheme 1 reveals that the two measurements actually compose a critical pair. As it is well known, gross errors in members of critical pairs are not identifiable. To break such criticality, a new measurement (active power flow $p_{20\text{-}15}$) on switching branch B2 is added to the measurement set, giving rise to metering scheme M.S. 2. Under the new conditions, the bad data identification and removal are correctly achieved as shown Table VIII.

The results of this experiment emphasize the importance of an adequate level of redundancy to allow the proper performance of the proposed algorithm. In particular, local redundancy conditions must prevent the occurrence of critical measurements and critical sets of measurements [15], since they are clearly detrimental to the performance of any bad data processing method.

TABLE VIII
BAD DATA PROCESSING ONLY

Inner Adjustment Method					
M.S.	*Measur. Identified*	r_i^N	$\hat{b}$	$J(\hat{\mathbf{x}})$ *Before*	$J(\hat{\mathbf{x}})$ *After*
1	P_{20}	10.007	33.244	131.89	44.67
2	$p_{15\text{-}16}$	11.586	14.385	150.38	4.269

Outer Adjustment Method					
M.S.	*Measur. Identified*	r_i^N	$\hat{b}$	$J(\hat{\mathbf{x}})$ *Before*	$J(\hat{\mathbf{x}})$ *After*
1	P_{20}	10.006	33.241	185.65	98.44
2	$p_{15\text{-}16}$	11.585	14.384	203.64	57.53

VII. CONCLUSIONS

This paper proposes an integrated method to estimate both state variables and network topology, which makes use of *a priori* state information to model switching branch statuses of a power network. The proposed approach allows the validation/correction of Network Processor results, and thus prevents the contamination of state estimates by topology errors. Several case studies presented in this paper with a subsystem of the IEEE 14-bus network indicate that, under adequate measurement redundancy levels, anomaly detection and identification can be accomplished whatever the type of the original modeling error, namely, topology error, bad data on analog measurements or a combination of both. The algorithm presents good self-healing characteristics, since it has been able to converge for a variety of distinct modeling errors, with bad data processing taking place in the second iteration starting from the flat start. Furthermore, numerical robustness is ensured by the properties of the orthogonal estimator.

REFERENCES

[1] A. Monticelli, *State Estimation in Electric Power Systems: A Generalized Approach*, New York: Springer, 1999, p. 394.

[2] N. Vempati, C. Silva, O. Alsaç and B. Bolt, "Topoloy Estimation", in *IEEE PES - Power Engineering Society General Meting*, vol. 1, p. 806-810, June, 2005.

[3] K. A. Clements and A. Simões Costa, "Topology error identification using normalized Lagrange multipliers", *IEEE Tans. Power Systems*, vol. 3, pp. 347-353, May. 1998.

[4] T. Yang, H. Sun and A. Bose."Transition to a two-level linear state estimator - part II: algorithm", *IEEE Trans. Power Systems*, vol. 26, pp. 54-62, Feb.,2011.

[5] F. Vosgerau, A. Simões Costa, K. A. Clements and E. M. Lourenço, "Power system state and topology coestimation", in *VIII IREP*, pp. 1-6, Buzios, Aug., 2010.

[6] J. Krstulovic, V. Miranda, A. Simões Costa and J. Pereira, "Towards an auto-associative topology states estimator", *IEEE Tans. Power Systems*, vol. 28, No. 3. pp. 3311-3318, Aug. 2013.

[7] E. Andreoli, A. Simões Costa and K. A. Clements, "Topology validation via simultaneous state & topology estimation with phasor data processing capability", in *18th Power System Computation Conference*, pp. 18-22, Wroclaw, Aug., 2014.

[8] P. Swerling, "Modern state estimation methods from the viewpoint of the method of least squares", *IEEE Trans. Automatic Control*, vol. AC-16, No. 6, pp. 707-719, Dec., 1971.

[9] E. M. Lourenço, L. B. Souza and A. Simões Costa. "A unified approach for bad data and topology error identification in generalized state estimation", in *16th Power System Computation Conference*, pp. 18-22, Glasgow, Jul., 2008.

[10] A. Simões Costa, M. E. Lourenço and F. Vieira, "Topology error identification for orthogonal estimators considering a priori state information", in *15th PSCC*, Liegem Belgium, session 26, paper 3, pp. 1-7, Aug. 2005.

[11] A. Simões Costa and V. H. Quintana, "An orthogonal row processing algorithm for power system sequential state estimation", *IEEE Transactions on Power Apparatus and Systems*, vol. PAS-100, pp.3791-3800, No. 8, 1981.

[12] N. Vempati, I. W. Slutsker and W. F. Tinney, "Enhancement to Givens rotations for power system state estimation", *IEEE Transactions on Power Systems*, vol. 6, pp.842-849, May, 1991.

[13] W. M. Gentleman, "Least squares computations by givens transformations without square roots", *Journal of the Inst. Math. Applics.*, vol. 12, pp. 329-336, 1973.

[14] A. Monticelli and A. Garcia. "Reliable bad data processing for real-time state estimation", *IEEE Transactions on Power Systems*, vol. PAS-102, n. 5, pp. 1143-1149, May, 1983.

[15] A. Simões Costa, E. M. Lourenço and A. Clements. "Power system topological observability analysis including switching branches", *IEEE Transactions on Power Systems*, vol. 17, n. 2, pp. 250-265, May, 2002.